INL/RPT-23-74814

Triply Periodic Minimal Surfaces Lattice Neutronics Scoping Studies

September 2023

William N. Fritsch[1]
Nicolas P. Martin[2]

[1]University of Tennessee, Knoxville
[2]Idaho National Laboratory

INL is a U.S. Department of Energy National Laboratory
operated by Battelle Energy Alliance, LLC

INL/RPT-23-74814

Triply Periodic Minimal Surfaces Lattice Neutronics Scoping Studies

William N. Fritsch[1]

Nicolas P. Martin[2]

[1]University of Tennessee, Knoxville
[2]Idaho National Laboratory

September 2023

Idaho National Laboratory

Reactor Physics Methods and Analysis, Nuclear Science and Technology Directorate

Idaho Falls, Idaho 83415

http://www.inl.gov

Prepared for the
U.S. Department of Energy
Office of Nuclear Energy
Under DOE Idaho Operations Office
Contract DE-AC07-05ID14517

Page intentionally left blank

ABSTRACT

Triply periodic minimal surfaces (TPMSs) have seen extensive research in heat exchanger development due to their enhanced heat transfer performance. When applied to reactor cores, TPMSs can more efficiently dissipate heat to the coolant, permitting increased power densities. The increased power density can be used to develop smaller reactors while retaining power output. Although TPMS core geometries promise enhanced heat transfer, the neutronic behavior of such geometries requires further inquiry. In this study, the neutron multiplication and buckling are compared between variations of the TPMS and traditional pincell core designs.

CONTENTS

FIGURES

TABLES

ACRONYMS

TPMS Triply Periodic Minimal Surface. 1

STL Stereolithographic. 2

PWR Pressurized Water Reactor. 3

SFR Sodium-cooled Fast Reactor. 3

SA/V Surface area to Volume ratio. 3

NSGA-II Non-dominated sorting genetic algorithm II. 4

Page intentionally left blank

1 INTRODUCTION

Reactor core design is heavily driven by fuel geometry, which can significantly impact neutron multiplication, depletion, and heat transfer capacity. Most reactor core geometries use pincell, plate, or pebble -based fuel. However, recent research has revealed improvements to such geometries can enhance reactor performance. The Massachusetts Institute of Technology proposed an annular fuel pellet geometry in 2001 that can increase power density by as much as 30%. [1] [2] Lightbridge's multilobed helical fuel geometry uses its characteristic twist to enhance turbulent mixing and increase safety margins. [3]

With recent advancements in additive manufacturing technology, research on complex geometries that were previously impractical to fabricate have gained popularity. Triply Periodic Minimal Surface (TPMS) is a particularly popular choice. TPMSs are tileable surfaces in three-dimensional space that locally minimize surface area. Figure 1 presents six examples of TPMS unit cells. TPMSs have seen use in lightweight, porous scaffolding, [4] which have been found in nature on the wings of butterflies and shells of sea urchins. [5] The peculiar shape of TPMSs have proven useful in heat exchanger and heat sink designs because their high surface area to volume ratio and inherent turbulent flow are ideal for heat transfer. [6] [7]

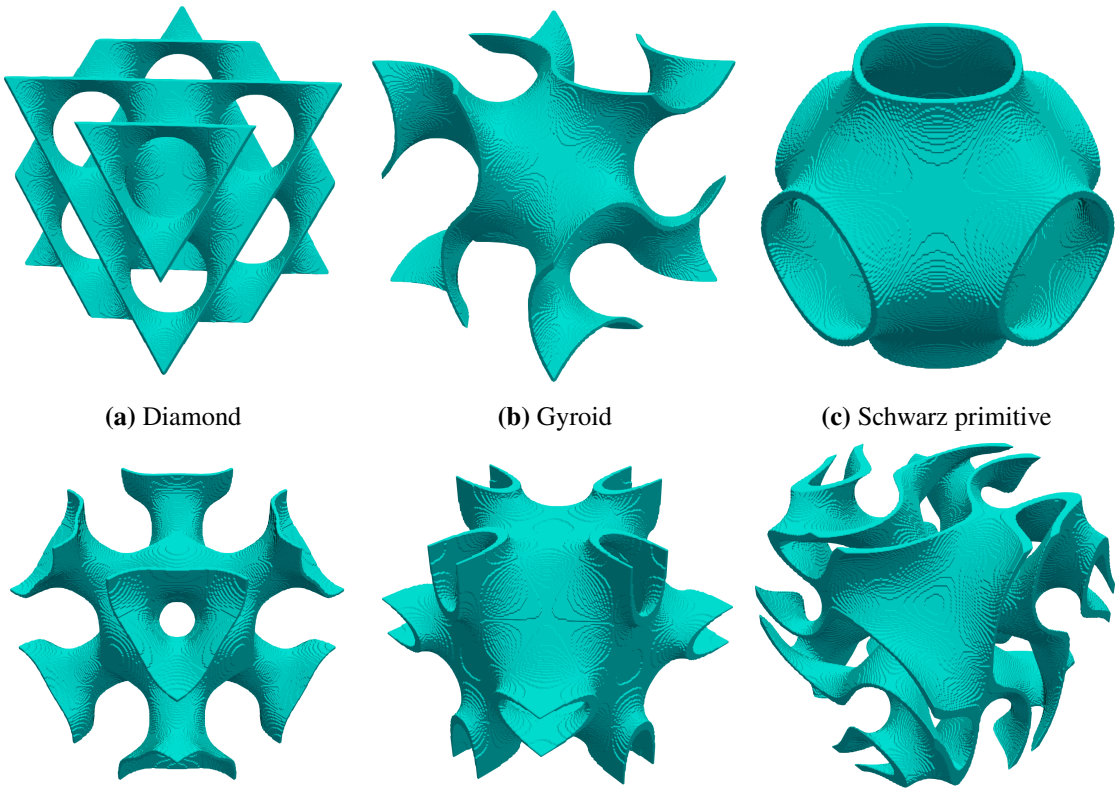

(a) Diamond **(b)** Gyroid **(c)** Schwarz primitive

(d) IWP **(e)** Neovius **(f)** P-Split

Figure 1: Six examples of TPMS unit cells. This study will focus on diamond and gyroid TPMS.

Nuclear power fundamentally relies on a heat source and a medium for transferring heat to a secondary circuit for electrical power. Ultimately, heat transfer plays a key role in reactor design, in which a TPMS reactor core design can contribute. Improved heat transfer permits increased power density. The potential for higher power density makes TPMS geometries attractive for microreactors and small modular reactors.

The thermal-hydraulic benefits of TPMSs are well recognised and summarized for instance in [8]. Very recently, the neutronic behavior of TPMS nuclear lattices was investigated [9], and the impact of key input parameters such as pitch and porosity on reactivity and spectrum were studied. The goal of this report is to expand the work performed in [9] and explore the neutronic behavior of various TPMS reactor core designs—for both fast and thermal spectrum reactors—and compare TPMSs to contemporary pincell core designs.

2 METHODS

This study examined two classes of TPMS geometries: solid fuel and sheet fuel. Solid fuel places the cladding along the TPMS surface, separating the fuel and coolant regions. Sheet fuel places the fuel along the TPMS surface itself, splitting the coolant into two regions. Figure 2 presents examples for solid-fuel and sheet-fuel geometries. A sheet-fuel TPMS has the advantage of a constant fuel thickness, unlike a solid-fuel TPMS. Fuel regions with an uneven thickness can introduce local temperature hot spots in the thicker regions, limiting power. Additionally, sheet-fuel geometries have two separate coolant channels, allowing the possibility of countercurrent coolant flow. These key features make the sheet-fuel TPMS stand out from a heat transfer perspective.

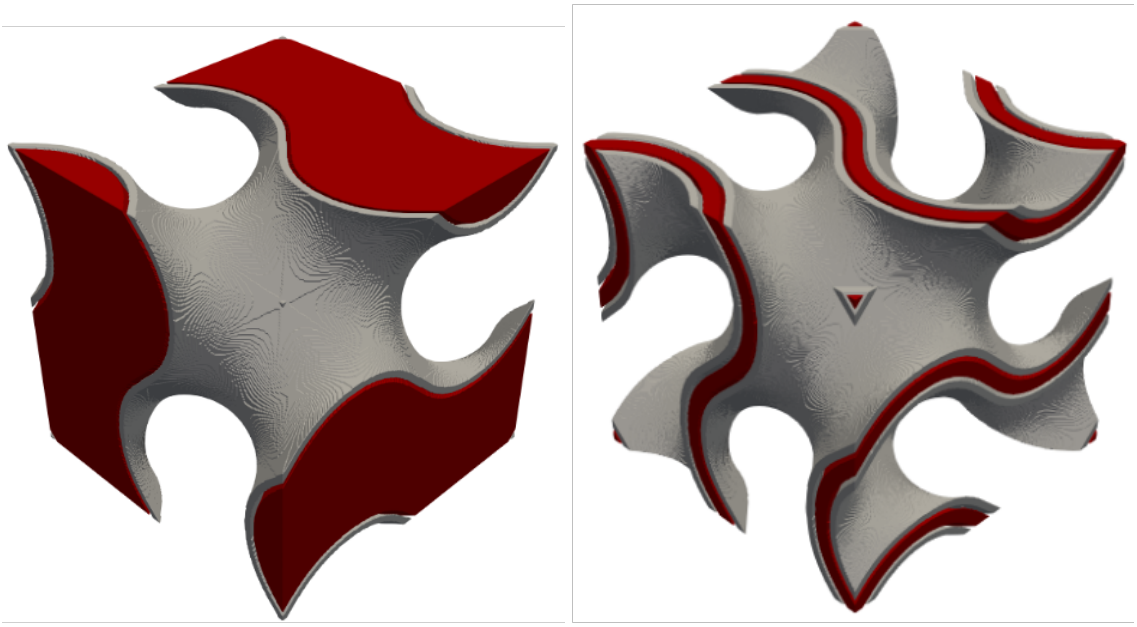

Figure 2: Solid fuel (left) and sheet fuel (right) gyroid TPMS geometries, with the fuel in red and cladding in gray.

2.1 TPMS Builder

TPMS Builder is a Python software developed to build TPMS core geometries. [10] TPMS Builder supports over 30 TPMS surface types, including popular geometries such as those presented in Figure 1. TPMS Builder constructs Stereolithographic (STL) files for the fuel, cladding, and coolant regions. TPMS Builder supports manipulating the *fuel relative density*—the volume of fuel divided by the volume of the unit cell. Cladding relative density and coolant relative density are also supported. TPMS Builder also features

functional grading for the unit cell pitch, fuel thickness, fuel relative density, and more. Figure 3 shows the fuel pitch and relative density grading.

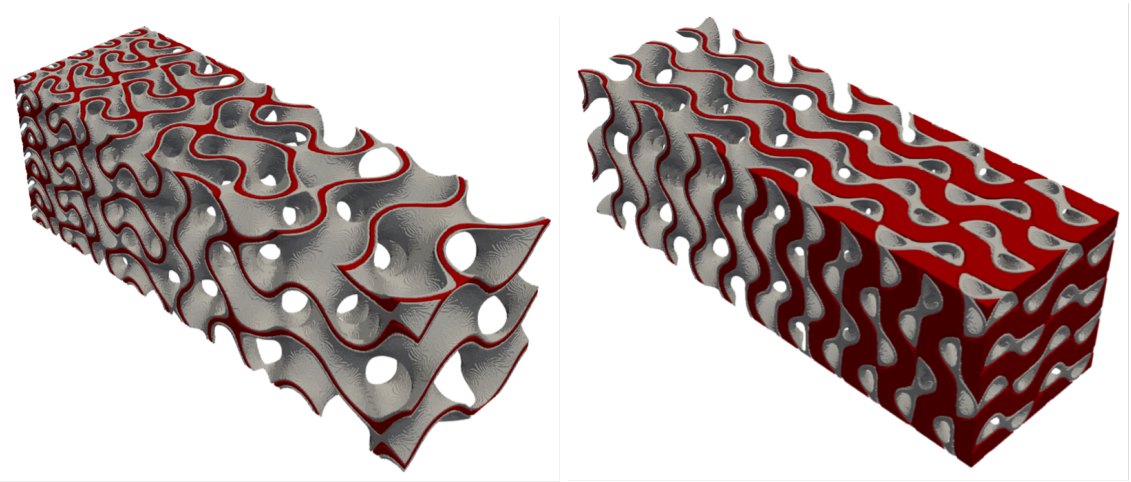

Figure 3: Unit cell pitch functional grading (left) and fuel relative density functional grading (right) applied to a gyroid sheet-fuel TPMS geometry.

2.2 Neutronics Simulation

Serpent 2 [11]—a Monte Carlo neutron transport software—is used to simulate the neutron transport in an infinitely repeating TPMS lattice. The STL geometry files from TPMS Builder are provided to Serpent 2 using the **`solid`** feature. [12] The TPMS geometries are compared against contemporary pincell designs.

Both thermal spectrum and fast spectrum reactors are modeled. The thermal spectrum reactor is based on a typical Pressurized Water Reactor (PWR): 5%-enriched UO_2 fuel, 0.6-mm-thick Zircalloy-4 cladding, and pressurized-water coolant. The comparative PWR assembly uses an infinitely repeating square pincell lattice. The fast spectrum reactor is based on a typical Sodium-cooled Fast Reactor (SFR): 19.5%-enriched U-10Zr fuel, 0.305-mm-thick HT9-SS cladding, and sodium coolant. The comparative SFR assembly uses an infinitely repeating hexagonal pincell lattice. In both models, the gas gap is ignored.

In this study, four variables are modified: unit cell pitch, fuel relative density, TPMS surface type, and whether sheet or solid fuel is used. Three measurements are considered: k_∞, the Surface area to Volume ratio (SA/V), and material buckling. The neutron multiplication factor, k_∞, determines the reactor fuel cycle duration. Longer fuel cycles reduce the frequency of scheduled shutdowns for refueling. SA/V is a simple criterion for measuring the heat transfer performance of a fuel geometry. Also, SA/V is highly correlated with heat transfer efficiency since power scales with fuel volume and convective heat transfer scales with surface area. Since SA/V is inversely proportional to pitch, the product of SA/V and pitch—which we will call χ—is constant with pitch. As such, SA/V can be found by dividing χ by the pitch.

Lastly, material buckling is a quantity describing neutron production, absorption, and transport within a reactor. Material buckling is used to approximate a reactor's critical core dimensions. Equation 1 defines material buckling, B_m^2, where Σ_a, Σ_f, ν, and D represent the absorption cross section, fission cross section, mean neutron production per fission, and diffusion coefficient, respectively. Serpent 2 internally calculates the one-group cross sections for Equation 1. Under the one-group diffusion theory, these cross sections successfully approximate the global neutronic behavior of a lattice geometry. When a core is critical, the material buckling is equal to the geometric buckling, B_g^2. Equation 2 gives the geometric buckling for a

cylindrical core with height, H, and radius, R. The geometric buckling is inversely proportional to the square of the reactor scale. To minimize a critical reactor's scale, material buckling should be maximized.

$$B_m^2 = \frac{\nu\Sigma_f - \Sigma_a}{D} \tag{1}$$

$$B_g^2 = \left(\frac{\pi}{H}\right)^2 + \left(\frac{2.405}{R}\right)^2 \tag{2}$$

2.3 Multiobjective Optimization

This study uses the Non-dominated sorting genetic algorithm II (NSGA-II) multiobjective optimization algorithm from the pymoo library [13] to find the optimal combination of pitch and relative density for a given TPMS geometry. The NSGA-II genetic algorithm balances performance and dispersion between multiple objectives. NSGA-II is chosen for its mixed-variable type support and popularity in multiobjective optimization. Since multiple objectives are considered, the results are presented as a Pareto front—a curve showing the trade-off between multiple objectives. Compiling the results as a Pareto front allows researchers to rank the performance of various fuel geometries without constraining one or more of the objectives. Each NSGA-II optimization is run for 20 generations, maintaining a population of 24 geometries.

2.4 Homogenization

The k_∞ of the TPMS geometries are compared to homogenized versions of the geometries using a ratio (heterogeneous k_∞ to homogenized k_∞). The homogenization ratios can be used to correct simplified models that assume homogeneity. The homogenized geometries are provided by a mixture using the volumetric fractions of the fuel, cladding, and coolant. The mixture is provided in Serpent 2 using the built-in **`mix`** feature using volumetric fractions found using TPMS Builder's relative density properties.

3 RESULTS

For the first part of this study, the diamond TPMS are compared to industry-standard pincell designs. Figure 4 (a), (b), and (c) show k_∞ versus fuel relative density and unit cell pitch for the sheet-fuel diamond TPMS, solid-fuel diamond TPMS, and pincell geometries in the PWR configuration. Figure 4 (d) plots the χ constants for each geometry. Figure 5 shows contour plots for the k_∞ of sheet-fuel TPMS versus unit cell pitch and fuel relative density for PWR and SFR models.

For both diamond TPMS and pincell cases, the fuel relative density must be around 30% or above for undermoderation—an important factor for power-temperature feedback. Figure 4 (d) shows that sheet-fuel TPMSs have a superior SA/V for a constant unit cell pitch. However, Figure 4 (a), (b), and (c) show that the optimal k_∞ have pitches of around 12, 6, and 3 cm for the sheet-fuel TPMS, solid-fuel TPMS, and pincell cases, respectively. Although diamond sheet fuel has an ideal SA/V, the unit cell pitches need to be higher for ideal neutronics.

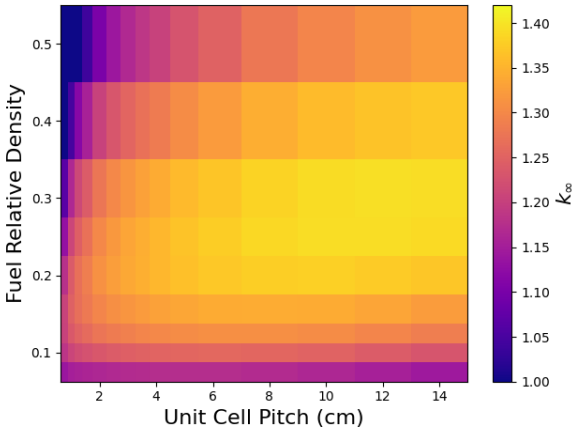

(a) Diamond sheet-fuel TPMS k_∞.

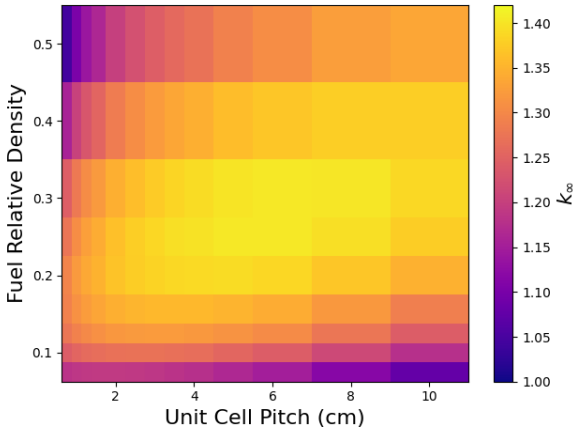

(b) Diamond solid-fuel TPMS k_∞.

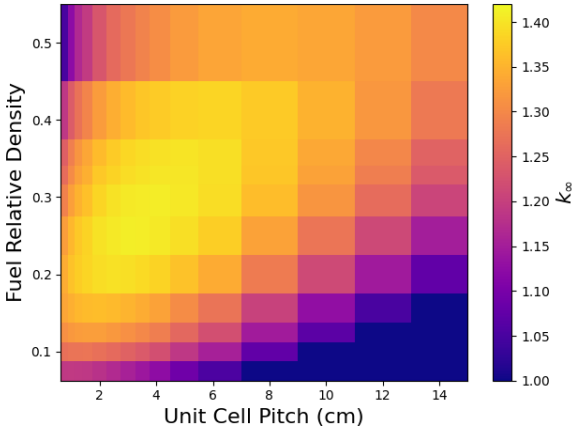

(c) Pincell lattice k_∞.

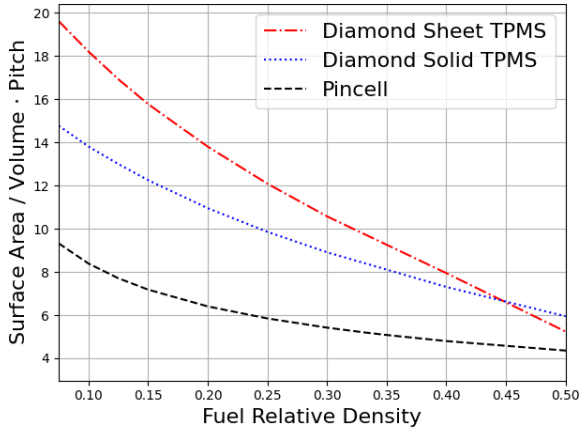

(d) χ constants for SA/V.

Figure 4: k_∞ versus cell and rod pitch and fuel relative density for (a) diamond sheet fuel, (b) diamond solid fuel, (c) and pincell geometries. SA/V constants, χ, are provided by the lower right plot (d) as a function of fuel relative density.

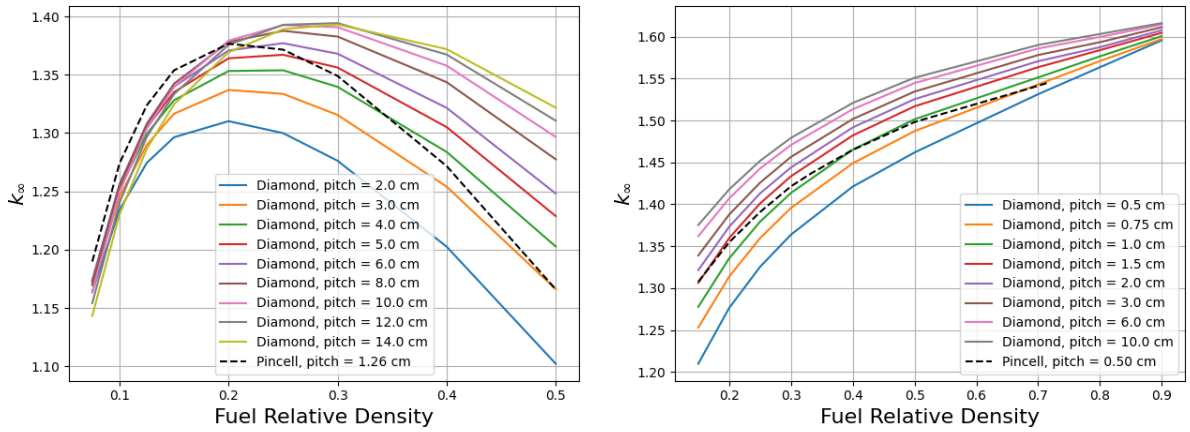

Figure 5: k_∞ versus fuel relative density for Diamond sheet-fuel TPMS and pincell fuel geometries for the PWR configuration (left) and the SFR configuration (right).

3.1 Multiobjective Optimization

The NSGA-II algorithm optimizes fuel relative density and unit cell pitch for the k_∞ and SA/V performance. Figure 6 presents the k_∞-SA/V Pareto fronts for gyroid and diamond solid-fuel and sheet-fuel TPMS and pincell geometries. Ultimately, the k_∞-SA/V performance is quite similar for pincell and TPMS geometries. For both PWR and SFR configurations, the solid-fuel TPMS outperform both pincell and sheet-fuel geometries when the SA/V ratio is high. As a reference, the a typical PWR has an SA/V of 4 cm^{-1} [14] and a typical SFR has an SA/V of 6–9 cm^{-1}. [15] The high SA/V standard for contemporary SFR designs are favorable for TPMS. Gyroid and diamond solid-fuel TPMSs perform similarly in both the PWR and SFR designs. The same conclusion can be made about gyroid and diamond sheet-fuel TPMSs. Overall, no significant differences are seen between TPMS surface types.

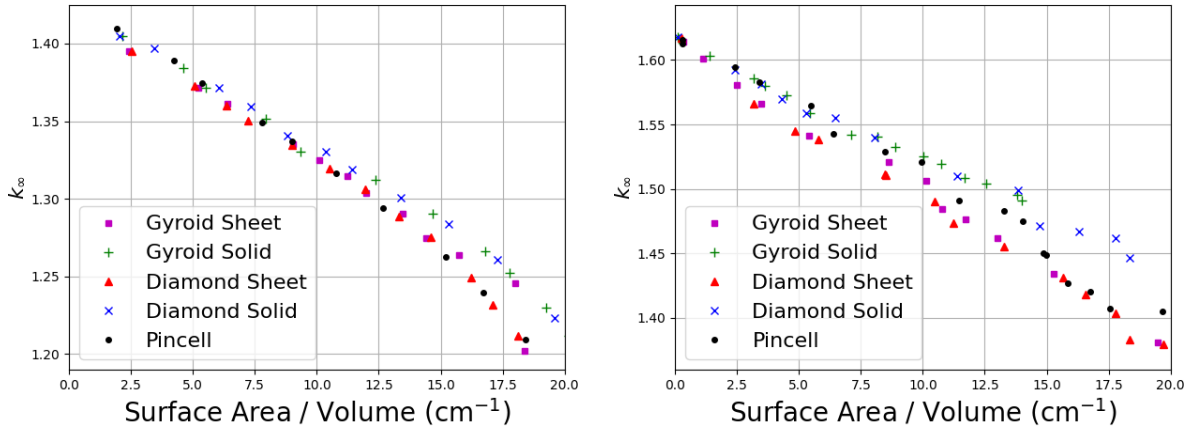

Figure 6: k_∞ versus SA/V Pareto front for pincell, diamond, and gyroid TPMS models. The PWR and SFR models are on the left and right, respectively.

3.2 Material Buckling

Figure 7 shows the Pareto front between material buckling and SA/V for the PWR and SFR cases. The PWR and SFR performances differ when considering material buckling. Sheet-fuel TPMSs perform better than pincell designs for the PWR case. For the SFR model, sheet-fuel TPMSs have much worse performance compared to pincell geometries. The reason behind this behavior requires further inquiry. Regardless, for the PWR model, both TPMS types have much better material buckling compared to pincell geometries, permitting smaller critical core geometries.

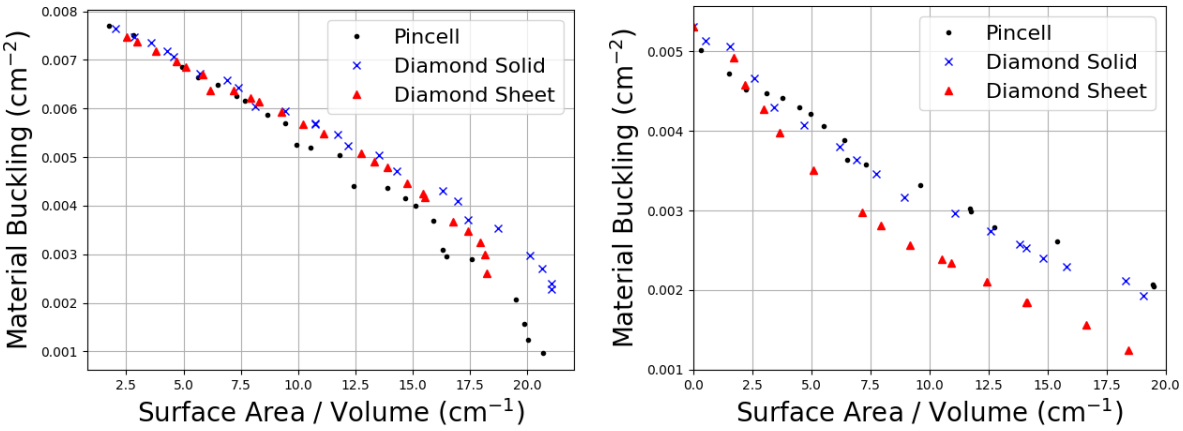

Figure 7: Material buckling versus SA/V Pareto front for pincell and diamond TPMS models. The PWR and SFR models are on the left and right, respectively.

The solid-fuel TPMS slightly outperforms the sheet-fuel TPMS in k_∞, SA/V, and material buckling for both the PWR and SFR designs. However, the benefits from constant fuel thickness and counter-current flow are not represented in the SA/V criterion for heat transfer performance. Furthermore, enhanced convection is a key feature in TPMS heat exchangers and heat sinks that is not represented in the SA/V criterion. A more in-depth heat transfer analysis is needed to identify the best TPMS geometry.

3.3 Homogenization

The homogenization ratios for the PWR and SFR configurations are provided in Tables 1 and 2. Table 1 shows that the PWR homogenization ratios increase with the fuel relative density when the unit cell pitch is high. The homogenization ratio is nearly constant for smaller unit cell pitches. Table 2 shows that the geometry has little influence on k_∞ as opposed to material composition. This result gives new insight into the SFR k_∞ and SA/V performance in Figure 6: the negative correlation between k_∞ and SA/V is mostly attributed to the material composition. Indeed, SA/V plays a large role in material composition since the cladding relative density increases with surface area.

Fuel Relative Density	Unit Cell Pitch (cm)					
	0.75	1.00	2.00	4.00	6.00	10.0
0.075	1.0127	1.0168	1.0244	1.0335	1.0341	1.0271
0.100	1.0146	1.0182	1.0296	1.0414	1.0442	1.0379
0.150	1.0173	1.0216	1.0355	1.0527	1.0592	1.0573
0.200	1.0177	1.0231	1.0399	1.0607	1.0701	1.0736
0.250	1.0182	1.0255	1.0432	1.0668	1.0801	1.0889
0.300	1.0166	1.0241	1.0452	1.0732	1.0874	1.1007
0.400	1.0122	1.0246	1.0486	1.0788	1.0999	1.1226
0.500	1.0072	1.0196	1.0447	1.0820	1.1067	1.1356

Table 1: k_∞ ratios between the diamond sheet-fuel TPMS and homogenized versions of the same geometry using the PWR thermal spectrum configuration.

Fuel Relative Density	Unit Cell Pitch (cm)					
	0.75	1.00	1.50	2.00	3.00	4.00
0.3	1.0013	1.0011	1.0014	1.0011	1.0012	1.0014
0.4	1.0006	1.0004	1.0007	1.0004	1.0008	1.0008
0.5	1.0006	1.0006	1.0006	1.0003	1.0007	1.0007
0.6	1.0005	1.0006	1.0006	1.0007	1.0004	1.0005
0.7	1.0005	1.0003	1.0004	1.0003	1.0004	1.0004
0.8	1.0001	1.0003	1.0001	1.0001	1.0005	1.0002
0.9	0.9997	1.0000	0.9999	1.0000	0.9999	0.9997

Table 2: k_∞ ratios between the diamond sheet-fuel TPMS and homogenized versions of the same geometry using the SFR fast spectrum configuration.

3.4 Burnup

Figure 8 plots k_∞ against burnup to determine potential depletion anomalies that may affect reactivity. Table 3 gives the fuel relative density and unit cell pitch parameters used for the burnup study. No significant reactivity anomalies appear for the thermal spectrum configuration—pincell, solid TPMS, and sheet TPMSs share a similar k_∞ versus burnup.

Geometry Type	Reactor Type	Fuel Relative Density	Unit Cell Pitch (cm)
Diamond Sheet	PWR	0.33	6.00
Diamond Solid	PWR	0.33	3.00
Pincell	PWR	0.33	1.26
Diamond Sheet	SFR	0.41	1.20
Diamond Solid	SFR	0.41	0.60
Pincell	SFR	0.41	0.57

Table 3: Fuel relative density and unit cell pitch parameters for the depletion calculations in Figure 8.

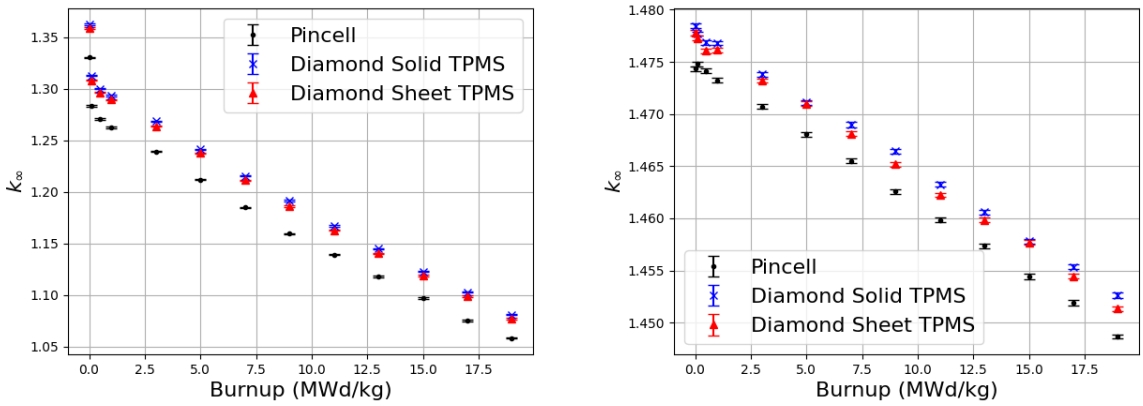

Figure 8: k_∞ versus burnup for the pincell, diamond solid-fuel TPMS, and diamond sheet-fuel TPMS for the PWR configuration (left) and SFR configuration (right).

4 CONCLUSION

Here, we studied the neutronic performance of TPMS fuel lattice geometries. TPMSs have excellent thermal-hydraulic properties that are ideal for dissipating heat to the coolant. These properties include inherent turbulent mixing and a large surface area, both of which improve convection. Serpent 2 simulated infinite TPMS lattice designs provided by TPMS Builder—a custom-built Python script for generating TPMS STL geometries. SA/V provided an estimate of heat transfer performance. Using multiobjective optimization on SA/V-k_∞ performance, a solid-fuel TPMS performs better than a sheet-fuel TPMS for both PWR and SFR configurations. However, SA/V is a elementary estimator of heat transfer performance, ignoring enhanced convection from turbulent mixing and fuel temperature uniformity from constant thickness.

Further research is required to determine the TPMS heat transfer performance using conductivity and thermal-hydraulic simulations. Such simulations can reveal the theoretical power density of TPMS geometries. Further study may include full-core optimization, spatially grading fuel relative density, unit cell pitch, and fuel composition to balance excess reactivity and leakage.

5 ACKNOWLEDGEMENTS

This work was supported through the Idaho National Laboratory Laboratory Directed Research and Development Program under the Department of Energy Idaho Operations Office Contract DE-AC07-05ID14517. This manuscript has been authored by Battelle Energy Alliance, LLC under Contract No. DE-AC07-05ID14517 with the U.S. Department of Energy. The United States Government retains and the publisher, by accepting the article for publication, acknowledges that the U.S. Government retains a nonexclusive, paid-up, irrevocable, world-wide license to publish or reproduce the published form of this manuscript, or allow others to do so, for U.S. Government purposes.

This research made use of the resources of the High Performance Computing Center at Idaho National Laboratory, which is supported by the Office of Nuclear Energy of the U.S. Department of Energy and the Nuclear Science User Facilities under Contract No. DE-AC07-05ID14517.

REFERENCES

[1] P. Hejzlar, M. Driscoll, and M. Kazimi, "Thermal hydraulics-I 4 high-performance annular fuel for pressurized water reactors," *Transactions of the American Nuclear Society*, vol. 84, pp. 192–194, 2001.

[2] M. Kazimi, P. Hejzlar, D. Carpenter, D. Feng, G. Kohse, W. Lee, P. Morra, H. No, Y. Ostrovsky, Y. Otsuka, P. Saha, E. Shwageraus, Z. Xu, Y. Yuan, J. Zhang, H. Feinroth, B. Hao, E. Lahoda, J. Mazzoccoli, and H. Hamilton, "High performance fuel design for next generation PWRs: Final report," 12 2012.

[3] J. Malone, A. Totemeier, N. Shapiro, and S. Vaidyanathan, "Lightbridge corporation's advanced metallic fuel for light water reactors," *Nuclear Technology*, vol. 180, no. 3, pp. 437–442, 2012.

[4] R. Pugliese and S. Graziosi, "Biomimetic scaffolds using triply periodic minimal surface-based porous structures for biomedical applications," *SLAS Technology*, vol. 28, no. 3, pp. 165–182, 2023. Bioprinting the Future.

[5] O. Al-Ketan and R. K. Abu Al-Rub, "Multifunctional mechanical metamaterials based on triply periodic minimal surface lattices," *Advanced Engineering Materials*, vol. 21, no. 10, p. 1900524, 2019.

[6] H. Peng, F. Gao, and W. Hu, "Design, modeling and characterization of triply periodic minimal surface heat exchangers with additive manufacturing," 08 2019.

[7] M. Khalil, M. I. Hassan Ali, K. A. Khan, and R. Abu Al-Rub, "Forced convection heat transfer in heat sinks with topologies based on triply periodic minimal surfaces," *Case Studies in Thermal Engineering*, vol. 38, p. 102313, 2022.

[8] K. Yeranee and Y. Rao, "A review of recent investigations on flow and heat transfer enhancement in cooling channels embedded with triply periodic minimal surfaces (tpms)," *Energies*, vol. 15, no. 23, 2022.

[9] N. Martin, S. Seo, S. B. Prieto, C. Jesse, and N. Woolstenhulme, "Reactor physics characterization of triply periodic minimal surface-based nuclear fuel lattices," *Progress in Nuclear Energy*, vol. 165, p. 104895, 2023.

[10] N. P. Martin and W. N. Fritsch, "TPMS builder." https://github.inl.gov/nicolas-martin/TPMS_builder.

[11] J. Leppänen, M. Pusa, T. Viitanen, V. Valtavirta, and T. Kaltiaisenaho, "The Serpent Monte Carlo code: Status, development and applications in 2013," *Annals of Nuclear Energy*, vol. 82, pp. 142–150, 2015. Joint International Conference on Supercomputing in Nuclear Applications and Monte Carlo 2013, SNA + MC 2013. Pluri- and Trans-disciplinarity, Towards New Modeling and Numerical Simulation Paradigms.

[12] A. Talamo, Y. Gohar, and J. Leppänen, "Serpent validation and optimization with mesh adaptive search on stereolithography geometry models," *Annals of Nuclear Energy*, vol. 115, pp. 619–632, 2018.

[13] J. Blank, "pymoo: Multi-objective optimization in Python." https://pymoo.org/index.html, 2022.

[14] NRC, "Westinghouse AP1000 design control document rev. 19." https://www.nrc.gov/docs/ML1117/ML11171A500.html, June 2011.

[15] “1.5-fast reactor fuels - NRC.” https://www.nrc.gov/docs/ML1914/ML19149A371.pdf, Mar 2019.